Fischer–Tropsch Synthesis

International Edition: DOI: 10.1002/anie.201603556
German Edition: DOI: 10.1002/ange.201603556

Highly Tunable Selectivity for Syngas-Derived Alkenes over Zinc and Sodium-Modulated Fe_5C_2 Catalyst

Peng Zhai, Cong Xu, Rui Gao, Xi Liu, Mengzhu Li, Weizhen Li, Xinpu Fu, Chunjiang Jia, Jinglin Xie, Ming Zhao, Xiaoping Wang, Yong-Wang Li, Qianwen Zhang, Xiao-Dong Wen,* and Ding Ma**

Abstract: *Zn- and Na-modulated Fe catalysts were fabricated by a simple coprecipitation/washing method. Zn greatly changed the size of iron species, serving as the structural promoter, while the existence of Na on the surface of the Fe catalyst alters the electronic structure, making the catalyst very active for CO activation. Most importantly, the electronic structure of the catalyst surface suppresses the hydrogenation of double bonds and promotes desorption of products, which renders the catalyst unexpectedly reactive toward alkenes—especially C_{5+} alkenes (with more than 50% selectivity in hydrocarbons)—while lowering the selectivity for undesired products. This study enriches C_1 chemistry and the design of highly selective new catalysts for high-value chemicals.*

Fischer–Tropsch synthesis (FTS), which converts natural gas/coal/biomass derived syngas (CO and H_2) into clean fuels and valuable chemicals, is of great academic and commercial importance.[1] The product distribution of FTS is so complex (from C_1 to C_{120}) that selective control of the reaction for certain components is a top priority and also the bottleneck of this process.[2] In general, the product contribution relies heavily on the type of catalyst and the specific reaction conditions. It is well known that alkenes are very valuable chemicals that are extensively used in the chemical industry. Very recently, Bao et al. reported that a bifunctional catalyst shows an unexpectedly high selectivity (80% of hydrocarbons) for lower olefins under 400 °C.[3] Later, it was shown that a combination of $ZnZrO_x$ (for methanol synthesis) and SAPO-34 (for methanol to olefin conversion) catalysts could dramatically increase the olefin selectivity as well.[4] However, the reaction window has to be precisely tuned for two or more reactions with different active phases, leading to significant challenges in engineering design.

Significantly, de Jong et al. reported that lower olefins can be selectively produced on S- and Na-modified Fe catalyst.[5] Since this report, direct synthesis of olefins from FTS using Fe-based catalysts has become an increasingly important research topic in the traditional FTS process.[6] Alkali metals are typically added to Fe-based catalyst as promoters to improve the catalytic performance by increasing the selectivity for lower olefins.[7] K is the most common promoter for increasing the hydrogenation barrier of the CH_x species and changing the pathway of methane formation, thereby enhancing olefin selectivity while suppressing the formation of methane.[8] Moreover, K could enhance the concentration of active surfaces intermediates,[9] atomic oxygen,[10] active facets,[11] or even directly take part in the reaction process by forming composites with Fe.[12] It is also reported that the addition of Na is sensitive to olefin production,[13] although the influence of Na on product selectivity is controversial and the way it functions is still unclear.[14] Moreover, Fe can form a solid solution or alloy with several different secondary metals, such as Cu, Mn, Cr, and Mo;[15] a bimetallic effect plays an important role in the multi-component systems.[16] The strong interaction between Zn and Fe inhibits the reduction of iron oxide but enhances the CO adsorption on the iron surface,[17] therefore making the catalyst favorable for production of long chain hydrocarbons.[18] However, the process is restricted by high methane productivity, as well as the associated water gas shift (WGS) activity, which produces large quantities of undesired CO_2.

Besides lower olefins, higher alkenes are important platform chemicals for producing highly valuable products, such as aromatic compounds and lubricating oil, as well as alcohols. However, in most cases the production of higher alkenes is associated with high CO_2 selectivity.[19] The full spectrum of alkene production is desirable, particularly with relatively low CO_2 selectivity. Herein, we report a Na- and Zn-modulated iron carbide catalyst, Fe-Zn-x Na, which shows an outstanding activity and high selectivity for alkenes (up to 79%) but modest CO_2 selectivity. By combining various in situ characterization approaches with density functional theory (DFT)

[*] P. Zhai, M. Li, W. Li, J. Xie, Prof. D. Ma
Beijing National Laboratory for Molecular Sciences, College of Chemistry and Molecular Engineering, Peking University
Beijing 100871 (China)
E-mail: dma@pku.edu.cn
C. Xu, M. Zhao, Prof. Q. Zhang
School of Chemical Engineering
Beijing Institute of Petrochemical Technology
Beijing 102617 (China)
E-mail: zhangqianwen@gmail.com
X. Fu, Prof. C. Jia
Key Laboratory for Colloid and Interface Chemistry, Key Laboratory of Special Aggregated Materials, School of Chemistry and Chemical Engineering, Shandong University
Jinan 250100 (China)
Dr. R. Gao, Dr. X. Liu, Dr. X. Wang, Prof. Y.-W. Li, Prof. X.-D. Wen
State Key Laboratory of Coal Conversion, Institute of Coal Chemistry
Chinese Academy of Sciences
P.O. Box 165, Taiyuan, Shanxi 030001 (P.R. China)
and
Synfuels China
Beijing 100195 (P.R. China)
E-mail: wxd@sxicc.ac.cn

Supporting information for this article can be found under: http://dx.doi.org/10.1002/anie.201603556.

calculations, a rationale for the structural modulation provided by Zn and the electronic modulation given by Na ions has been clearly revealed, which is vital for understanding complicated multicomponent FTS catalytic systems and contributes toward the development of highly selective FTS processes.

Fe-Zn-x Na catalysts were synthesized by a coprecipitation/washing method. Unless otherwise specified, Fe and Zn have the same concentration on Fe-Zn-x Na catalysts (Na concentration is described as x%; $x = 3.4$, 0.81, 0.36%; catalyst without Na (x = 0%) is termed Fe-Zn). Catalysts without Zn were also prepared (Fe-1.2 Na, with 1.2% Na). Calcined Fe-1.2 Na catalysts were washed up to 60 times to generate Fe catalyst (Na-free).

Fe-Zn-x Na catalysts have similar XRD patterns (Figure 1 a), being a mixture of ZnO and $ZnFe_2O_4$, although Fe-Zn-3.4 Na presents relatively strong ZnO diffractions. Other than $ZnFe_2O_4$, no additional phases of Fe were observed, indicating the robustness of interaction between Zn and Fe. The spinel structure promotes superior intimacy between Fe and Zn, leading to an alteration in the size of the crystal. Catalysts with Zn have relatively small crystals (8.4–13.0 nm with Zn vs. 15.4–19.6 nm without; Supporting Information, Table S1). This indicates that Zn changes the size of the coprecipitated Fe species. We measured the CO uptake of the reduced catalysts (Supporting Information, Table S2). The catalyst with Zn has a larger exposed surface than that without, which is in good agreement with XRD observations. The elemental mapping results indicated that Fe, Zn, and Na are nearly uniformly distributed in the calcined sample, but Zn enriched areas were sometimes observed as well (Supporting Information, Figure S1). XRD patterns show that the dominant phases are $ZnFe_2O_4$ and ZnO.

The catalytic performance was evaluated at 340 °C (Table 1). Remarkably, by comparing the Fe-Zn-0.81 Na catalyst with Fe-1.2 Na (the two catalysts have a similar Na content), a drastic increase in CO conversion was observed (from 48.7 to 77.2%). The difference is clearer when we compare the mass-specific activity (Figure 1 b). The stable activity of Fe-1.2 Na is around 0.72 $mol_{CO}\,g_{Fe}^{-1}\,h^{-1}$, while that of Fe-Zn-0.81 Na is 2.4 $mol_{CO}\,g_{Fe}^{-1}\,h^{-1}$, which is three times higher than the former. However, the selectivity of the two catalysts was similar. The trend also holds for catalysts without Na (Table 1, entries 4 and 6). Therefore, in line with XRD and CO adsorption results, this means that Zn works as a structural promoter, the addition of which leads to smaller Fe crystals and therefore more exposed surface sites. Consequently, the mass-specific activity is dramatically increased.

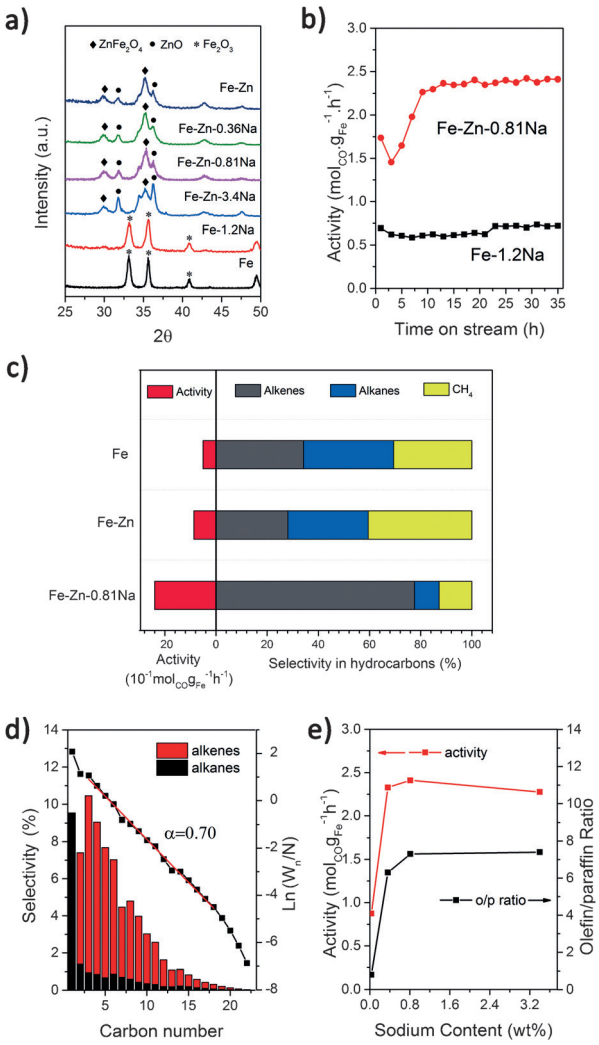

Figure 1. a) XRD patterns for the calcined catalysts. b) The comparison of activity vs. time between Fe-Zn-0.81 Na and Fe-1.2 Na catalysts. c) The activity and product distribution on Fe-Zn-0.81 Na, Fe-Zn, and Fe catalysts. Reaction conditions: catalysts (20 mg), 340 °C, 2.0 MPa, syngas ($CO:H_2:CO_2:Ar = 24:64:8:4$; 20 mL min^{-1}). d) The detailed hydrocarbon product distribution obtained over Fe-Zn-0.81 Na. e) Catalytic activity and o/p molar ratio as a function of Na content.

Table 1: The catalytic performance of various catalysts in the FTS reaction.[a]

Entry	Catalysts	Conv. [%]	CO_2 (Sel.)	Selectivity [C mol%]			o/p[b]	α	Activity [$mol_{CO}\,g_{Fe}^{-1}\,h^{-1}$]
				CH_4	C_2-C_4	C_{5+}			
1	Fe-Zn-3.4 Na	63.0	22.5	8.6	22.6	46.3	7.4	0.68	2.2
2	Fe-Zn-0.81 Na	77.2	23.8	9.7	25.9	40.6	7.2	0.69	2.4
3	Fe-Zn-0.36 Na	82.7	25.9	11.7	26.5	35.9	6.3	0.67	2.3
4	Fe-Zn	34.1	33.1	27.1	29.9	9.9	0.8	0.54	0.87
5	Fe-1.2 Na	48.7	21.9	7.5	22.8	47.8	8.3	0.71	0.72
6	Fe	32.7	31.2	21.0	28.4	19.4	1.6	0.59	0.51

[a] Reaction conditions: catalyst (20 mg), syngas ($CO:H_2:CO_2:Ar = 24:64:8:4$; 20 mL min^{-1}), 2.0 MPa, 340 °C. Pretreated with H_2/N_2 (5%) at 300 °C for 4 h. The data is collected at 40 h. [b] the ratio of olefin to paraffin.

It is worth noting that most of the Fe-based catalysts for alkene production have a strong tendency to produce a large amount of CO_2,[20] and the CO_2 selectivity of Fe catalyst for alkene production in previous reports is normally above 36% at high temperature.[21] Therefore, the suppression of CO_2 formation is a major task for FTS research at high temperature. Significantly, besides the higher activity, Fe-Zn-*x*Na catalysts show relatively low selectivity towards CO_2 compared to the Fe-Zn catalyst (Table 1, entries 1–4). The selectivity towards CO_2 can be suppressed to $<25\%$ by adding 8% CO_2 into the feed, which means that a larger proportion of the available carbon resource in syngas has been fixed into hydrocarbons.

Besides lower CO_2 selectivity, the formation of saturated hydrocarbons was almost inhibited and methane was well-suppressed by the Fe-Zn-0.81 Na catalyst (Figure 1 c), with the dominant product being the desired alkenes. The selectivities for all alkenes and C_{5+} alkenes were as high as 79% (88% if methane was not considered) and 51% among all the hydrocarbons (Figure 1 c,d). We noticed that for a catalyst with a similar Na concentration but without Zn (Fe-1.2 Na), although the activity is much lower than that for the Fe-Zn-0.81 Na catalyst, similar product distributions were observed (Table 1); that is, sparse C_1 products and high selectivity for alkenes. As expected, this means that Na plays a vital role in selective conversion of syngas into alkenes. A series of samples with the same Zn content but different Na loadings ranging from 0–3.4% were compared. The addition of Na changed the reduction as well as the carburization behavior of the catalyst (Supporting Information, Figures S2–5). Significantly, the dependence of the activity and olefin/paraffin ratio on the concentration of Na of the Fe-Zn-x Na catalysts is shown in Figure 1 e. For catalyst without Na (Fe-Zn), the steady state activity is lowest (that is, 0.87 $mol_{CO}\,g_{Fe}^{-1}\,h^{-1}$). Steady state activity increased significantly with the addition of Na, passing through a maximum at a Na concentration of 0.81%. Upon further increase of the Na content, a slow decrease of activity was observed. Indeed, a small amount of Na may act as an electronic donator to Fe or iron carbide, which facilitates the activation of CO and leads to a higher FTS activity. Most importantly, there was an obvious correlation between selectivity of products and Na concentration (Figure 1 e). The olefin/paraffin molar ratio (o/p ratio) was only 0.8 on Fe-Zn, suggesting that the majority of hydrocarbons correspond to alkanes when Na is absent from the catalyst. However, the o/p ratio drastically increased with an increase of Na concentration; for catalyst with 0.36% Na the o/p ratio reached 6.3. This ratio goes as high as 7.4 when the loading of Na is 3.4%. At the same time, the existence of Na not only suppressed the formation of alkane, but also inhibited the WGS reaction to some extent, and subsequently improved the carbon efficiency significantly (Table 1).

We used STEM/EDX to study the distributions of different elements in Fe-Zn-0.81 Na catalyst after 3 h of reaction, which already reached the best performance in steady-state FTS (Figure 2). Clearly, phase segregation occurred because of crystalline phase transformation of the sample from $ZnFe_2O_4$ and ZnO, into Fe_5C_2, Fe_3O_4, and ZnO; Zn and Fe species were separated with a clear boundary. To our surprise, the distribution of Na is very interesting. On ZnO it is homogeneously distributed both in the surface and the bulk, but on iron carbide it was only observed on the external surface of the crystals. As catalytic reactions take place on the surface of this catalyst, the surface modulation of Na on Fe species is the key for the altered catalytic behavior. To study the effect of electronic modulation of Na on Fe catalyst, we compared the evolution of electronic character in the near-surface region of Fe-Zn-0.81 Na and Fe-Zn catalysts during the activation/reaction process using in situ X-ray photoelectron spectroscopy (XPS; Figure 3 a,b). The catalysts were treated in 2.0 MPa syngas at different temperatures (RT, 200, 300, and 340 °C). The sample treated at 340 °C underwent a further 150 min heat treatment at 340 °C to generate the 340 °C-3 h sample. Whereas the R-340 °C-3 h sample was generated after reduction of the Fe-Zn catalyst in pure hydrogen at 400 °C for 2 h, followed by reaction with syngas at 340 °C for 3 h. After treatment the samples were transferred to the measurement chamber without exposure to air. Below 300 °C, Fe-Zn shows a characteristic $Fe^{III}\,2p_{3/2}$ peak at 710.6 eV,[22] indicating that most of the Fe present remains in a ferric oxide form at these temperatures. However, for Fe-Zn-0.81 Na we observed a 0.6 eV shift toward lower binding energy, although the treatment temperature was the same, suggesting that charge transfer from Na ions to the surface iron oxides is possible. When the treatment temperature reached 340 °C, the peak shifted toward lower binding energies that correspond to the formation of Fe^{II} species. Upon prolongation of the treatment time to 3 h, a new peak at 705.2 eV appeared, which is characteristic of iron carbide in

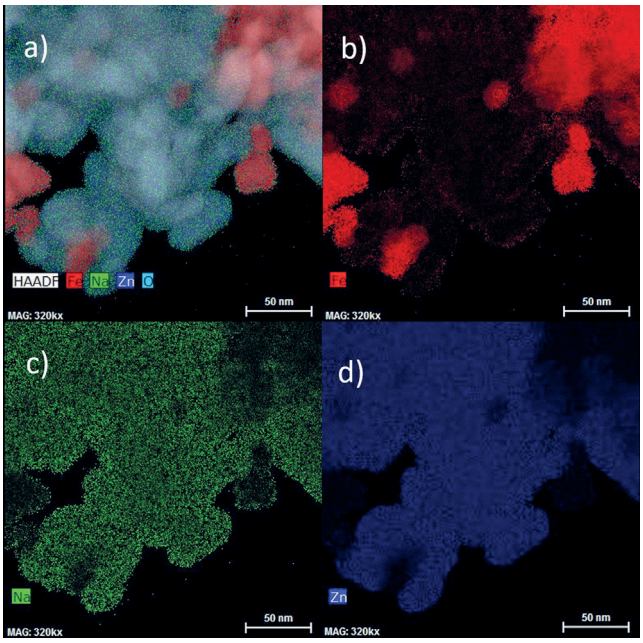

Figure 2. a–d) The elemental mapping of Fe-Zn-0.81 Na catalyst after reaction for 3 hours. Fe (red), Na (green), Zn (blue). Scale bar: 50 nm. Reaction conditions: catalyst (20 mg), 340 °C, 2.0 MPa, syngas ($CO:H_2:CO_2:Ar = 24:64:8:4$), pretreated with H_2/N_2 (5%) at 300 °C for 4 h.

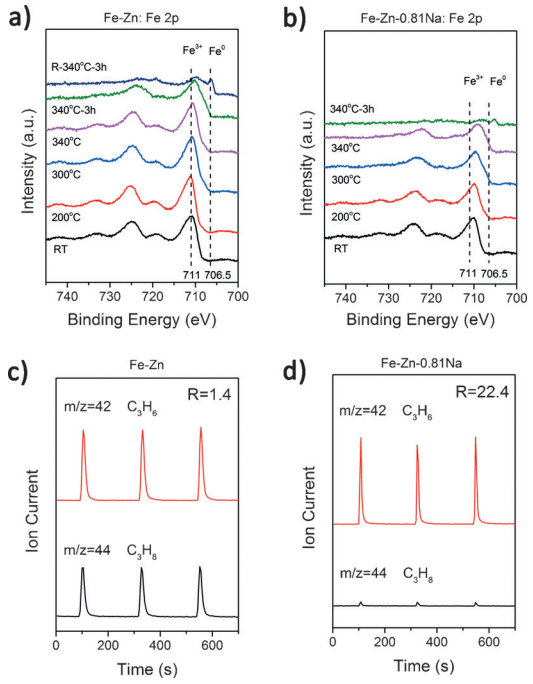

Figure 3. Fe 2p XPS spectra of a) Fe-Zn and b) Fe-Zn-0.81 Na treated in syngas (20 mL min^{-1}) at different temperatures. (a) R-340 °C-3 h (blue line) indicates that the sample was reduced in pure hydrogen (20 mL min^{-1}) at 400 °C for 2 h and then treated in syngas (20 mL min^{-1}, 2.0 MPa) for 3 hours at 340 °C. c,d) Transient response curves obtained during pulses of 250 µl diluted C_3H_6 (7.5 % C_3H_6, 2.5 % Ar, 90 % N_2) into a flow of pure H_2 (20 mL min^{-1}) at 340 °C, over Fe-Zn (c) and Fe-Zn-0.81 Na catalysts (d). Before the pulse reaction, the samples (20 mg) were pretreated with H_2 (20 mL min^{-1}, 400 °C) and reacted in syngas (20 mL min^{-1}, 2.0 MPa) at 340 °C for 20 min. R = ratio of C_3H_6/C_3H_8 peak area detected by MS.

a zero valent state. However, this peak is more than 1 eV lower (705.2 vs. 706.5 eV) than the standard iron carbide sample,[23] suggesting the formation of electron-rich iron carbide species. By comparison, the iron carbide species formed on the Fe-Zn catalyst still has a binding energy of 706.4 eV. Indeed, from the plotted charge density difference based on DFT calculations (Supporting Information, Figures S6 and S7), it can be seen that delocalized electrons are transferred from Na to the interface of iron when the Na ion is distributed on the surface of Fe_5C_2, making the surface iron carbide species electron rich. Furthermore, the electron transfer can be confirmed by the computed Bader charge of the Fe atom in Fe_5C_2 and Na_2O/Fe_5C_2 (+0.52 vs. +0.34). Although it has long been speculated that electron transfer might occur between alkali promoter and iron,[24] in the present study we provide the intuitive evidence experimentally and theoretically.

One of the key factors affecting the o/p ratio is the weakening of hydrogenation ability of the working catalyst surface and thus inhibition of hydrogenation of the formed alkenes on the surface of that catalyst.[25] To verify our theoretical hypothesis, we used a pulse experiment to explore the reactivity of alkenes on the iron carbide with and without Na modulation (Figure 3 c,d). The catalysts were firstly reacted in syngas at 340 °C for 20 min to reach a steady-state, before switching to a flow of H_2 (20 mL min^{-1}) at the same temperature. Propene was pulsed into the reactor and the effluent (propene and propane) were detected by mass spectrometer, thereby allowing the percentage of hydrogenated alkene to be determined. Clearly, a much narrower pulse width of propene was observed on the Fe-Zn-0.81 Na catalyst than that for Fe-Zn (half width: 7 s vs. 13 s), demonstrating the weaker adsorption, and thus the faster desorption, of alkenes on the surface of the Na-modified iron carbide catalyst. More importantly, for Fe-Zn at least 36 % of the propene was hydrogenated to propane, suggesting that the unmodified iron carbide catalyst promotes the alkene hydrogenation reaction well. To our surprise, the formation of propane was almost totally inhibited with catalyst containing 0.81 % Na (Fe-Zn-0.81 Na; see Figure 3 d). This result indicates that Na not only accelerates alkene desorption on the surface, but also suppresses the secondary hydrogenation of alkenes. A similar phenomenon was observed when propylene was replaced by ethylene in this experiment (Supporting Information, Figure S8). Compared with propylene, a small amount of ethylene was hydrogenated to ethane on Fe-Zn-0.81 Na under these condition, which is in accordance with the fact that propylene is more easily obtained than ethylene on iron catalyst (Figure 1 d).

To understand the dramatic effect of Na on the selectivity for FTS products, we carried out reaction mechanism calculations on iron carbide catalysts. Based on the experimental characterization results, two surface models (Supporting Information, Figure S6) for $Fe_5C_2(111)$ and $Na_2O/Fe_5C_2(111)$ were constructed to represent the iron catalyst without Na or Fe-*x* Na catalyst. In Figure 4 a, the calculation results showed that the adsorption energy of C_3H_6 was weakened by Na from −0.82 eV (without Na) to −0.55 eV (with Na) on the same Fe adsorption site, which is in good agreement with the experimental observations. The first hydrogenation ($C_3H_{6+}H \rightarrow C_3H_7$) barrier was similar (0.67 vs. 0.66 eV) for both catalysts. Comparably, the hydrogenation barrier was higher than the desorption energy of C_3H_6 on Na_2O/Fe_5C_2 (111) (0.66 > 0.55 eV), indicating that C_3H_6 is more easily desorbed from the surface instead of being hydrogenated. However, desorption of C_3H_6 cannot occur on the clean surface of Fe_5C_2 (111) because its hydrogenation barrier is lower than the desorption barrier (0.67 < 0.82 eV). This observation is in line with the prediction of Norskov et al. for the acetylene hydrogenation reaction.[27] From a frontier orbital point of view, the adsorption of olefins (C = C) corresponds to a major interaction between the surface z^2 band and the π_σ/π_σ^* state, as shown in Figure 4 b. The doping Na breaks the symmetry of such a z^2 band on the surface, leading to weakening of the adsorption of olefins. The DFT calculations suggested that the main effect of Na on iron carbide was the electronic structure modulation. The existence of Na would suppress the hydrogenation of olefins by weakening the adsorption of olefins and further enhancing the o/p ratio; this hypothesis is confirmed by our experimental results.

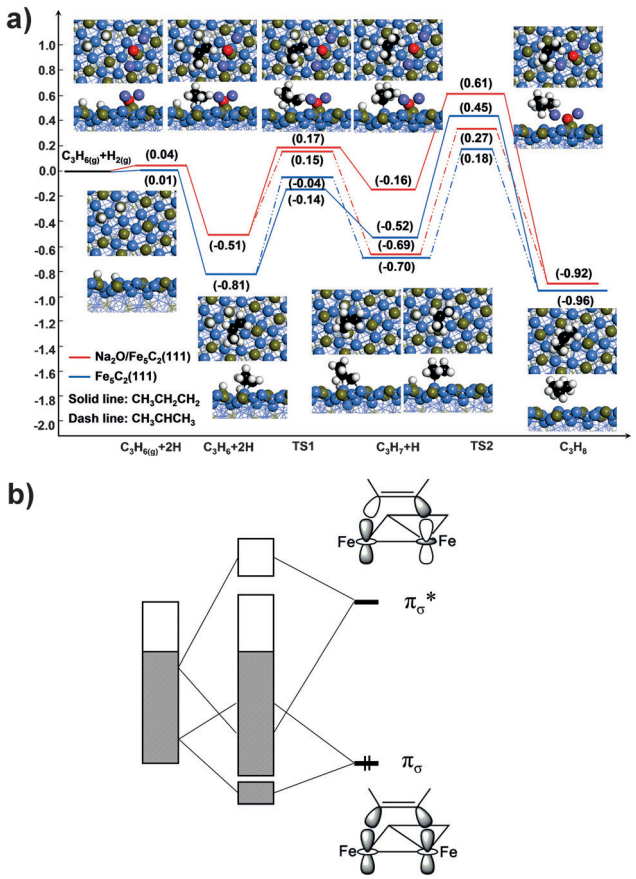

Figure 4. a) The reaction path for propene hydrogenation into propane on Fe_5C_2 (111) (blue line) and Na_2O/Fe_5C_2 (111) (red line) surfaces, the adsorption energies of H_2 and C_3H_6 include the zero point energy (ZPE) and entropy correction at 340 °C and 2.0 MPa. Atom key: Fe (blue), C (brown), Na (purple), and O (red); the C atoms of C_3H_6 are in black for clarity. b) Schematic describing the orbital interactions between olefins and surfaces, modified from [26].

Acknowledgements

This work received financial support from the Natural Science Foundation of China (21473003, 21222306, 21473229 and 91545121) and 973 Project (2013CB933100). The XAS experiments were conducted at the Beijing Synchrotron Radiation Facility (BSRF) and Shanghai Synchrotron Radiation Facility (SSRF). We thank Siyu Yao for XAFS data discussion. X.-D.W. also acknowledges National Thousand Young Talents Program of China, Hundred-Talent Program of Chinese Academy of Sciences. The computational resources for the project were supplied by the Tianhe-2 in Lvliang, Shanxi and National Supercomputing Center in Shenzhen.

Keywords: CO hydrogenation · heterogeneous catalysis · iron catalysts · olefins · sodium dopant

How to cite: *Angew. Chem. Int. Ed.* **2016**, *55*, 9902–9907
Angew. Chem. **2016**, *128*, 10056–10061

[1] a) M. E. Dry, *Catal. Today* **2002**, *71*, 227–241; b) A. Y. Khodakov, W. Chu, P. Fongarland, *Chem. Rev.* **2007**, *107*, 1692–1744.
[2] Q. H. Zhang, J. C. Kang, Y. Wang, *ChemCatChem* **2010**, *2*, 1030–1058.
[3] F. Jiao, J. J. Li, X. L. Pan, J. P. Xiao, H. B. Li, H. Ma, M. M. Wei, Y. Pan, Z. Y. Zhou, M. R. Li, S. Miao, J. Li, Y. F. Zhu, D. Xiao, T. He, J. H. Yang, F. Qi, Q. Fu, X. H. Bao, *Science* **2016**, *351*, 1065–1068.
[4] K. Cheng, B. Gu, X. L. Liu, J. C. Kang, Q. H. Zhang, Y. Wang, *Angew. Chem. Int. Ed.* **2016**, *55*, 4725–4728; *Angew. Chem.* **2016**, *128*, 4803–4806.
[5] H. M. T. Galvis, J. H. Bitter, C. B. Khare, M. Ruitenbeek, A. I. Dugulan, K. P. de Jong, *Science* **2012**, *335*, 835–838.
[6] a) H. M. T. Galvis, K. P. de Jong, *ACS Catal.* **2013**, *3*, 2130–2149; b) J. Z. Lu, L. J. Yang, B. L. Xu, Q. Wu, D. Zhang, S. J. Yuan, Y. Zhai, X. Z. Wang, Y. N. Fan, Z. Hu, *ACS Catal.* **2014**, *4*, 613–621; c) X. Q. Chen, D. H. Deng, X. L. Pan, Y. F. Hu, X. H. Bao, *Chem. Commun.* **2015**, *51*, 217–220.
[7] J. C. Park, S. C. Yeo, D. H. Chun, J. T. Lim, J. I. Yang, H. T. Lee, S. Hong, H. M. Lee, C. S. Kim, H. Jung, *J. Mater. Chem. A* **2014**, *2*, 14371–14379.
[8] a) Y. Yang, H. W. Xiang, Y. Y. Xu, L. Bai, Y. W. Li, *Appl. Catal. A* **2004**, *266*, 181–194; b) M. S. Luo, R. J. O'Brien, S. Q. Bao, B. H. Davis, *Appl. Catal. A* **2003**, *239*, 111–120; c) B. Graf, H. Schulte, M. Muhler, *J. Catal.* **2010**, *276*, 66–75.
[9] N. Lohitharn, J. G. Goodwin, *J. Catal.* **2008**, *260*, 7–16.
[10] M. A. Petersen, M. J. Cariem, M. Claeys, E. van Steen, *Appl. Catal. A* **2015**, *496*, 64–72.
[11] C. F. Huo, B. S. Wu, P. Gao, Y. Yang, Y. W. Li, H. J. Jiao, *Angew. Chem. Int. Ed.* **2011**, *50*, 7403–7406; *Angew. Chem.* **2011**, *123*, 7541–7544.
[12] J. Gaube, H. F. Klein, *Appl. Catal. A* **2008**, *350*, 126–132.
[13] a) K. Cheng, V. V. Ordomsky, B. Legras, M. Virginie, S. Paul, Y. Wang, A. Y. Khodakov, *Appl. Catal. A* **2015**, *502*, 204–214; b) J. B. Li, H. F. Ma, H. T. Zhang, Q. W. Sun, W. Y. Ying, D. Y. Fang, *Fuel Process. Technol.* **2014**, *125*, 119–124.
[14] a) H. M. T. Galvis, A. C. J. Koeken, J. H. Bitter, T. Davidian, M. Ruitenbeek, A. I. Dugulan, K. P. de Jong, *J. Catal.* **2013**, *303*, 22–30; b) X. An, B. S. Wu, W. J. Hou, H. J. Wan, Z. C. Tao, T. Z. Li, Z. X. Zhang, H. W. Xiang, Y. W. Li, B. F. Xu, F. Yi, *J. Mol. Catal. A* **2007**, *263*, 266–272.
[15] a) E. de Smit, F. M. F. de Groot, R. Blume, M. Havecker, A. Knop-Gericke, B. M. Weckhuysen, *Phys. Chem. Chem. Phys.* **2010**, *12*, 667–680; b) M. C. Ribeiro, G. Jacobs, R. Pendyala, B. H. Davis, D. C. Cronauer, A. J. Kropf, C. L. Marshall, *J. Phys. Chem. C* **2011**, *115*, 4783–4792; c) H. L. Wang, Y. Yang, J. A. Xu, H. Wang, M. Y. Ding, Y. W. Li, *J. Mol. Catal. A* **2010**, *326*, 29–40.
[16] a) V. R. Calderone, N. R. Shiju, D. Curulla-Ferre, S. Chambrey, A. Khodakov, A. Rose, J. Thiessen, A. Jess, G. Rothenberg, *Angew. Chem. Int. Ed.* **2013**, *52*, 4397–4401; *Angew. Chem.* **2013**, *125*, 4493–4497; b) V. R. Calderone, N. R. Shiju, D. C. Ferre, G. Rothenberg, *Green Chem.* **2011**, *13*, 1950–1959.
[17] a) J. L. Zhang, S. P. Lu, X. J. Su, S. B. Fan, Q. X. Ma, T. S. Zhao, *J. CO2 Util.* **2015**, *12*, 95–100; b) P. Sharma, T. Elder, L. H. Groom, J. J. Spivey, *Top. Catal.* **2014**, *57*, 526–537; c) S. Li, A. Li, S. Krishnamoorthy, E. Iglesia, *Catal. Lett.* **2001**, *77*, 197–205.
[18] S. L. Soled, E. Iglesia, S. Miseo, B. A. Derites, R. A. Fiato, *Top. Catal.* **1995**, *2*, 193–205.
[19] H. J. Wan, B. S. Wu, C. H. Zhang, H. W. Xiang, Y. W. Li, *J. Mol. Catal. A* **2008**, *283*, 33–42.
[20] a) Y. Liu, J. F. Chen, J. Bao, Y. Zhang, *ACS Catal.* **2015**, *5*, 3905–3909; b) A. C. J. Koeken, H. M. T. Galvis, T. Davidian, M. Ruitenbeek, K. P. de Jong, *Angew. Chem. Int. Ed.* **2012**, *51*, 7190–7193; *Angew. Chem.* **2012**, *124*, 7302–7305.
[21] S. Krishnamoorthy, A. W. Li, E. Iglesia, *Catal. Lett.* **2002**, *80*, 77–86.

[22] E. de Smit, M. M. van Schooneveld, F. Cinquini, H. Bluhm, P. Sautet, F. M. F. de Groot, B. M. Weckhuysen, *Angew. Chem. Int. Ed.* **2011**, *50*, 1584 – 1588; *Angew. Chem.* **2011**, *123*, 1622 – 1626.
[23] C. Yang, H. B. Zhao, Y. L. Hou, D. Ma, *J. Am. Chem. Soc.* **2012**, *134*, 15814 – 15821.
[24] M. C. Ribeiro, G. Jacobs, B. H. Davis, D. C. Cronauer, A. J. Kropf, C. L. Marshall, *J. Phys. Chem. C* **2010**, *114*, 7895 – 7903.
[25] a) N. S. Govender, F. G. Botes, M. H. J. M. de Croon, J. C. Schouten, *J. Catal.* **2014**, *312*, 98 – 107; b) J. F. Li, X. F. Cheng, C. H. Zhang, Y. Yang, Y. W. Li, *J. Mol. Catal. A* **2015**, *396*, 174 – 180.
[26] R. Hoffmann, *Solids and Surfaces: A Chemist's View of Bonding in Extended Structures*, Wiley-VCH, Weinheim, **1989**, p 110.
[27] J. K. Nørskov, T. Bligaard, J. Rossmeisl, C. H. Christensen, *Nat. Chem.* **2009**, *1*, 37 – 46.

Received: April 12, 2016
Revised: June 17, 2016
Published online: July 22, 2016

